ELSEVIER

Physica B 318 (2002) 365–371

PHYSICA B

www.elsevier.com/locate/physb

Evidence of a weak electronic density distortion in polymerized A_1C_{60} (A = K and Rb) compared to pristine C_{60}

M. Marangolo[a,*], Ch. Bellin[a], G. Loupias[a], S. Rabii[b], S.C. Erwin[c], Th. Buslaps[d], A. Issolah[e]

[a] *Laboratoire de Minéralogie-Cristallographie de Paris, Univ. Paris VI et VII, URA CNRS 7590, case 115, 4 pl. Jussieu, 75252 Paris Cedex 05, France*

[b] *Department of Electrical Engineering, University of Pennsylvania, Philadelphia, PA 19104-6390, USA*

[c] *Complex Systems Theory Branch, NRL, Washington, DC 20375, USA*

[d] *European Synchrotron Radiation Facility (ESRF), BP 220, 38043 Grenoble Cedex, France*

[e] *Laboratory Physique Quantique, Univ. De Tizi-Ouzou, 1500 Tizi-Ouzou, Algeria*

Abstract

Compton profile measurements on K_1C_{60} and Rb_1C_{60} and C_{60} powders have been carried out using inelastically scattered photons. We compare experimental Compton Profile Difference (CPD) of K_1C_{60} and that of C_{60} with the corresponding calculated results, obtained from ab initio self-consistent field calculations of the energy band structure. This permits us to isolate the contribution of the distortion of the C_{60} orbitals for each compound and to compare them. In previous paper, we have shown that for A_nC_{60} compounds this approach leads to a good agreement between theory and experiment. In this paper, we show that it is not the case for K_1C_{60}. The distortion contribution is overestimated by calculations leading to a CPD narrower than the experimental one. Furthermore similar measurements performed on heavy ions intercalated compounds (Rb_1C_{60}) show clearly that CPD depends on the number of ions and not on their nature. We think that our results corroborate the conclusions of a very small distortion of C_{60} molecules in the polymerized phase obtained by neutron diffraction experiments by Fox et al. (Chem. Phys. Lett. 249 (1996) 195).

Keywords: Fullerenes; Compton; Intercalation; Polymerization

1. Introduction

In solid C_{60} and in most of its intercalated compounds, the intermolecular separation is mainly determined by van der Waals interactions. Some years ago some exceptions have been found in which C_{60} molecules are linked by covalent bonds. Pure C_{60} polymerizes under pressure and A_1C_{60} (A = K, Rb) compounds have a polymeric form at room temperature with an orthorhombic crystal structure in which C_{60} molecules form chains.

Stephens et al. [1] have reported an X-ray investigation of the structure of A_1C_{60} (A = K, Rb) compounds and have provided a direct evidence for a covalent bonding between neighboring C_{60} molecules. This model involves (1) strongly linked and distorted fullerene molecules

*Corresponding author. Fax: +33144273785.
E-mail address: marangol@1mcp.jussieu.fr (M. Marangolo).

0921-4526/02/$ - see front matter
PII: S0921-4526(02)00806-2

(interball bond distance similar to bond lengths within undistorted C_{60} molecules, (2) long C–C intramolecular bond lengths (1.9 Å), (3) short C–C intramolecular bond lengths (1.32 Å).

In 1996 Fox et al. [2] obtained Pair Distribution Functions from powder neutron diffraction measurements. They claimed that the geometry of the interfullerene linkages is similar to Stephens's, but the distortion of the C_{60} molecules is much weaker.

To our knowledge this discussion is still open. This is surprising since these systems have attracted the interest of many groups because of their electronic and magnetic properties. The consequences of the one-dimensional structure of these systems have been strongly debated up to some years ago: Chauvet et al. [3] have shown that Rb_1C_{60} is a quasi-1D conductor, where spin or charge density wave instabilities lead to an insulating ground state. On the other hand, Erwin et al. [4] performed calculations on a crystal structure close to that of Stephens. They found that the electronic and magnetic properties of the polymerized phase remain strongly three-dimensional.

Our experimental Compton scattering study has been motivated by the strong distortion expected in these polymerized compounds with respect to pristine C_{60}. Surprisingly, the measured distortion is very weak, corroborating the Fox's results.

2. Experimental and theoretical procedure

We have already reported on our investigation of momentum density in C_{60} [5], K_6C_{60} [6] and in A_nC_{60} ($n = 3, 4$) [7]. In this work, we extend our experimental and theoretical studies to K_1C_{60} and Rb_1C_{60}. The wave functions obtained from ab initio energy band calculation of these compounds are used to calculate directional Compton profiles, which are the projections of electron momentum density along specific directions. Experimentally, inelastic scattering of X-rays from powder samples is used to measure an averaged Compton profile. Experimental and theoretical studies of electronic structure in momentum space are particularly suited for investigation of valence electrons in solids due to their extended nature. Furthermore, the incoherent nature of the X-rays inelastic scattering makes this approach ideally suited in the cases where high quality samples are not available.

Since the information provided by Compton scattering about the ground-state electron distribution can be directly related to the Fourier expansion of the wave function, this approach can be used as a direct probe of the quality of the calculated wave functions.

Sections 3 and 4 present Compton scattering and the theoretical approach. Section 5 presents the experimental procedures, including sample preparation and characterization. Results and discussions are presented in Section 6 and conclusions given in Section 7.

3. Compton scattering method

When photons are inelastically scattered by electrons, the wavelength shift of the photons can be related to scattering angle and the initial momentum of electrons through conservation of energy and momentum. The resulting shift is given by

$$\Delta\lambda = \frac{2h}{mc}\sin^2\left(\frac{\varphi}{2}\right) + \frac{2\lambda_1}{mc}\sin\left(\frac{\varphi}{2}\right)q, \tag{1}$$

where φ is the scattering angle, λ_1 the incoming beam wavelength and q is the value of the initial electron momentum in the scattering direction.

The first term, i.e., the Compton shift, is simply the result of photons scattered by electrons at rest. The information about the ground state momentum density is contained in the second term, which is a broadening of the Compton peak due to the motion of the electrons.

In the impulse approximation (IA), one assumes that the scattering is fast enough so that the interaction potential can be regarded as unchanged during the process. Within this approximation, the Compton profile is defined as

$$\begin{aligned} J(q, \mathbf{e}) &= \int n(\mathbf{p})\delta(\mathbf{p}\cdot\mathbf{e})\,\mathrm{d}\mathbf{p} \\ &= \int \chi^*(\mathbf{p})\chi(\mathbf{p})\delta(\mathbf{p}\cdot\mathbf{e} - q)\,\mathrm{d}\mathbf{p}, \end{aligned} \tag{2}$$

where **e** is the unit vector along the scattering vector **K**, $n(\mathbf{p})$ is the electron momentum density and $\chi(\mathbf{p})$ is the wave function of the electron in momentum space, i.e., the Fourier transform of the wave function in real space [8–10]. Throughout the remainder of this paper we shall use atomic units (a.u.), for which $= m = 1$.

4. Theoretical approach

The electronic structures of C_{60} [11] and K_1C_{60} [4] were calculated within the local density approximation using the Ceperly Adler exchange-correlation functional. The Kohn–Sham equations were solved using the ab initio linear-combination-of-atomic-orbitals (LCAO) method. The localized orbitals were expanded on a set of Gaussian-orbital basis functions. The basis set for carbon-included 4s-type and 3p-type Gaussian functions while for potassium it contained five s-type and four p-type functions. The calculations were self-consistent, with no restrictions on the form of charge density or potential. Due to the large size of the unit cell, a single k-point (Γ) was sufficient to achieve convergence in the Brillouin zone (BZ) integration. The details of the formalism are given in Ref. [12].

The calculated ground-state wave functions are represented by their planewave expansion,

$$\psi_{n,\mathbf{k}}(\mathbf{r}) = \sum_{\mathbf{G}} C_{n,\mathbf{k}}(\mathbf{G}) \exp[\mathrm{i}(\mathbf{k}+\mathbf{G})\cdot\mathbf{r}], \tag{3}$$

where **G**'s are reciprocal lattice vectors. The large sizes of the primitive unit cells for these compounds result in very short lengths of the reciprocal lattice vectors. Therefore, the number of G's necessary to obtain convergence in this sum is large. Using this expansion in Eq. (2) results in the following form for the directional Compton profile:

$$J(q,\mathbf{e}) = \frac{1}{N}\sum_{n}\sum_{\mathbf{k}}\sum_{\mathbf{G}}\left|C_{n,\mathbf{k}}(\mathbf{G})\right|^2 \times \delta((\mathbf{k}+\mathbf{G})\cdot\mathbf{e}-\mathbf{q})\vartheta(E_n - E_f). \tag{4}$$

The summation **G** is over all the reciprocal lattice vectors for which the $C_{n,\mathbf{k}}(\mathbf{G})$'s are non-negligible. Summation **k** is over the symmetry-reduced sector of the BZ of each compound, using a tetrahedral interpolation method [13]. The volume of this irreducible sector of the BZ is divided into tetrahedra by choosing a grid of **k** points. The actual wave functions are calculated at each grid point and a linear interpolation is carried out for $|C_{n,\mathbf{k}}(G)|^2$ within each tetrahedron.

The summation n is over the occupied states. The function θ cuts off this summation at the Fermi energy in the case where the material is a metal or a semi-metal. Since the measurements are performed on powder samples, the comparison is made with the average theoretical profile obtained by calculating four directional profiles.

5. Experimental procedure

5.1. Sample characterization

C_{60} powder from the Hoechst company is used in this study. The powder that contains some impurities, in particular sulfur, is meticulously purified. This purification consists of a very slow outgassing under high vacuum, from room temperature to 400°C. The temperature is progressively increased, so that the pressure remains lower than 10^{-5} mm Hg. The process takes four to six weeks. XANES (X-ray absorption near edge structures) study was used to show that this treatment has completely removed all impurities, included oxygen [14]. After outgassing, the powder is transferred under a pure argon atmosphere to avoid any oxygen contamination.

Rb_1C_{60} and K_1C_{60} samples were prepared in L. Forro's group in Lausanne. These samples were prepared by solid-state reaction of stoichiometric quantities of alkali metal and sublimed high-purity C_{60} powder.

The quality of the samples has been checked by electron spin resonance (ESR) and NMR measurements. Since samples coming from the same group in Lausanne have been measured by Chauvet et al. [15] (ESR spectra of Rb_1C_{60}) and by Brouet et al. [16] (NMR spectra of K_1C_{60} and Rb_1C_{60}), we state that our samples present the same high standard of quality.

5.2. Experimental set-up

The experiments on K_1C_{60} and Rb_1C_{60} were carried out using the Compton spectrometer of the high-energy beamline (Insertion Device 15B) [17] at the European Synchrotron Radiation Facility in Grenoble, France. The synchrotron radiation beam was monochromatized to select 55.8 eV photons and then focused on a powder sample. The powder was kept in a 1 mm diameter Lindemann capillary under argon atmosphere. The collected Compton spectra were energy analyzed using the Ge 440 Bragg reflections. Each spectrum achieved 10^6 counts at the Compton peak.

The energy dependent resolution function is deduced from the full-width at half-maximum (FWHM) of the thermal diffuse scattering (TDS) peak, which was 0.25 atomic units of momentum (a.u.).

5.3. Data processing

After subtracting the background, the raw data were corrected for wavelength-dependent terms such as absorption (in the sample and analyzer), detector efficiency, and analyzer reflectivity predicted by kinematical theory [18]. The wavelength scale was then converted into a momentum scale. The spectra were normalized to the number of electrons per carbon atom.

In order to obtain the valence electrons Compton profile, the core electrons profile (K 3p excluded) was subtracted from the total measured profile. Under the impulse approximation, the core contribution is obtained from atomic wave functions. This approximation is valid only if the energy ΔE transferred from the photon to the ejected electron is large compared with the binding energy of the electron [19].

The potassium 3p core electrons will be treated as a "pseudo-core" as described in the next section. After removing the core contributions, the remaining profile is normalized to the number of valence electrons per carbon atom, i.e. 4 in C_{60}.

In these experiments, IA Hartree–Fock Compton profiles for potassium and rubidium core electrons were subtracted from the total measured profiles [20].

6. Results and discussion

Band structure calculations, in general and those for C_{60} compounds in particular, are usually performed in order to obtain quantitative information about the charge distribution and Fermi surfaces (where applicable) [11,12]. Our interest here is in the momentum space representation of the wave function, $\chi(p)$, leading to the electron momentum density and the related Compton profiles. While the calculated momentum density is obviously less intuitive than the real space charge density, it has the advantage of (1) providing an integrated view of the characteristics of the electrons, (2) is sensitive to the contributions of the more delocalized electrons (valence and conduction), and (3) can be directly related to the results of Compton scattering experiments, thereby providing an excellent test for the calculated wave functions.

The utility of this approach has already been demonstrated in intercalation compounds of graphite [21,22] and more recently for C_{60} [5] and K_6C_{60} [6] and A_nC_{60} ($n = 3, 4$) [7].

6.1. Compton profile analysis

In the following, we will consider the experimental and theoretical Compton Profiles of $K_1C_{60}-C_{60}$ (normalized to 6 electron of C_{60}). The difference profile is the result of three contributions:

1. *The* K 3p *electron contribution*: The area of this contribution to the CP is normalized to the number of K 3p electrons per carbon atom, i.e. 0.05 in the low-energy side of CP ($q > 0$).
2. *The conduction profile*: This contribution is due to the electrons in the upper complex of three bands originating from the lowest unoccupied t_{1u} molecular orbitals in C_{60}. This complex forms the conduction band in K_nC_{60}, which becomes completely filled for $n = 6$. It is

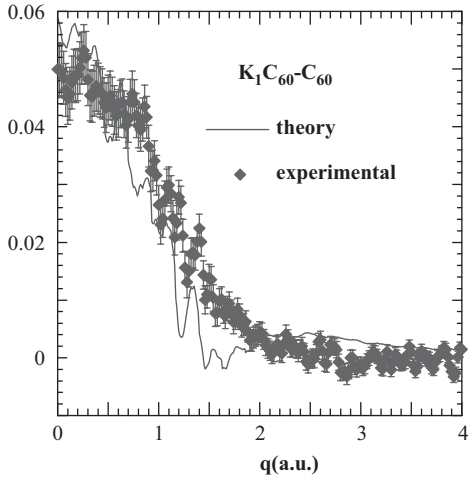

Fig. 1. Comparison between the experimental and theoretical valence Compton profiles of K_1C_{60}–C_{60}. The theoretical profiles (—) is convoluted with the experimental resolution. The experimental results are represented by filled diamonds.

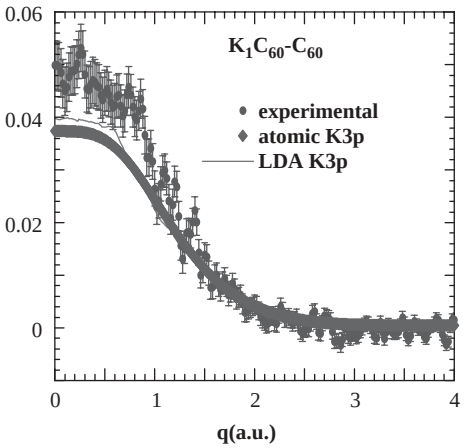

Fig. 2. Comparison between the experimental theoretical valence Compton profiles of K_1C_{60}–C_{60} with atomic and LDA K 3p Compton profiles.

normalized to 0.008333 in the low-energy side of CP ($q > 0$).

3. *The distortion profile*: This contribution is related to the distortion of the pristine C_{60} electronic density due to the presence of the K^+ ions. The net area under this profile is zero.

The comparison of experimental and theoretical K_1C_{60}–C_{60} Compton profile (with their own correct normalization) is shown in Fig. 1. The overall agreement between theory and experiment is not good if compared to similar spectra of K_3C_{60}, K_4C_{60} [7] and K_6C_{60} [6].

We notice that, in the K_1C_{60}–C_{60} case, the experimental Compton profile is lower in the 0.0–0.8 a.u. region, broader for the 0.8 a.u. $< q <$ 2 a.u. region and lower in the 2–4 a.u region, compared to the theory.

In Fig. 2, we compare the K_1C_{60}–C_{60} Compton profile with the atomic K 3p contribution [20] and the contribution of K 3p (pseudo-core) obtained by band structure calculations.

Two points must be considered:

1. The atomic K 3p and the "pseudo-core" K 3p contributions shown in Fig. 2 are very similar indicating that the electron momentum density of these occupied states is only slightly modified in the intercalated solid phase.
2. The theoretical CPD in Fig. 1 is the sum of the "pseudo-core" K 3p contribution, the conduction profile (always positive) and the distortion profile. We notice that the experimental CPD shows the same slope of K 3p profile for $q > 1$ a.u. (The difference at low q-values is due to the conduction contribution). We can conclude that the theoretical distortion contribution leading to the narrow calculated CPD shown in Fig. 1 is not present in the real material.

In other words ab initio calculations performed with the Stephens et al. configuration overestimate the valence electron distortion in the solid.

Also for Rb_1C_{60} compounds these considerations are valid: one can compare the Rb_1C_{60}–C_{60} CPD, shown in Fig. 3, with the experimental K_1C_{60}–C_{60} CPD (Fig. 1). The comparison corroborates a result already obtained for A_nC_{60} compounds [7]: "The CPDs of A_nC_{60} compounds do not depend on the nature of the intercalated ions but rather on their number." The trends in the experimental heavy ions intercalated CPDs reproduce the figures discussed previously for K_1C_{60}.

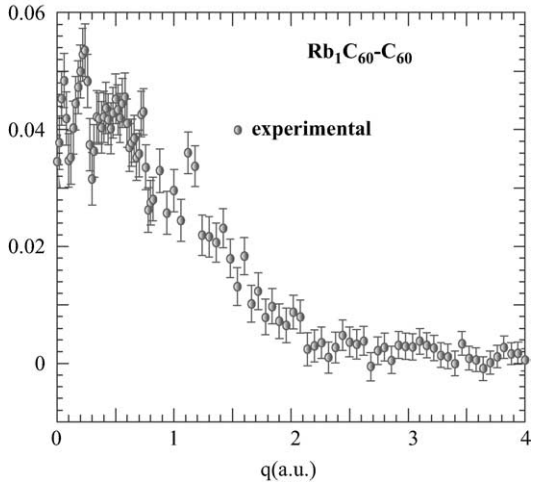

Fig. 3. Experimental Compton profile of $Rb_1C_{60}-C_{60}$.

7. Conclusions

We have measured the Compton Profiles of A_1C_{60} (A = K,Rb) and obtained CPD between these compounds and pristine C_{60}. In the case of potassium intercalated compounds, the simulation of CPDs by ab initio calculations do not describe the main trends of the experimental results.

K_1C_{60} presents a distortion that is less important than expected in calculation performed in the Stephens et al. configuration.

We stress that for K_3C_{60}, K_4C_{60} [7] and K_6C_{60} [6], we have obtained a better agreement between theory and experiment using a similar procedure.

Furthermore similar measurements performed on heavy ion intercalation compounds (Rb_1C_{60}) show clearly that the CPD depends on the number of ions and not on their nature.

We notice that powder neutron diffraction measurements performed by Fox et al. [2] had already shown that "Although the interfullerene linkages are similar to those proposed previously and suggest the formation of covalent intermolecular bonds, the present results involve considerably less distortion on the C_{60} molecules than reported by Stephens et al."

We believe that our results corroborate the Fox's thesis since the expected distortion obtained by ab initio calculations on the Stephens et al. configuration is not observed in K_1C_{60} and Rb_1C_{60}.

We hope that band structure calculations in the Fox [2] configuration will be performed in the future in order to compare with our experimental results.

Acknowledgements

We would like to thank P. Suortti for useful discussions. We are grateful to L. Forro (Physics Dept./IGA Ecole Polytechnique Federale de Lausanne Switzerland) V. Brouet and C. Hérold, J.F. Marêché, Ph. Lagrange (LCSM, Univ. Nancy I, BP 239, 54506 Vandoeuvre-Cedex, France) for providing samples.

References

[1] P.W. Stephens, G. Bortelet, G. Faigel, M. Tegze, A. Jànossy, S. Pekker, G. Oszlanyi, L. Forro, Nature 370 (1994) 636.
[2] J.R. Fox, G.P. Lopinski, J.S. Lannin, G.B. Adams, J.B. Page, J.E. Fischer, Chem. Phys. Lett. 249 (1996) 195.
[3] G. Chauvet, L. Oszlànyi, P.W. Forro, M. Stephens, G. Tegze, Faigel, A. Jànossy, Phys. Rev. Lett. 72 (1994) 2721.
[4] S. Erwin, G.V. Krishna, E.J. Mele, Phys. Rev. B 51 (1995) 7345.
[5] J. Moscovici, G. Loupias, S. Rabii, S. Erwin, A. Rassat, C. Fabre, Europhys. Lett. 31 (2) (1995) 87.
[6] M. Marangolo, J. Moscovici, G. Loupias, S. Rabii, S. Erwin, C. Hérold, J.F. Marêché, Ph. Lagrange, Phys. Rev. B 58 (1998) 7593.
[7] M. Marangolo, Ch. Bellin, G. Loupias, S. Rabii, S.C. Erwin, Th. Buslaps, Phys. Rev. B 60 (1999) 17084.
[8] P. Eisenberger, P.M. Platzman, Phys. Rev. A 2 (1970) 415.
[9] M.J. Cooper, Rep. Prog. Phys. 48 (1985) 415.
[10] L. Mendelsohn, V.H. Smith, in: B. Williams (Ed.), Compton Scattering, McGraw-Hill, New York, 1977.
[11] S.C. Erwin, in: W.E. Billups, M.A. Ciufolini (Eds.), Buckminsterfullerenes, VCH, New York, 1993, p. 217.
[12] S.C. Erwin, M.R. Pederson, W.E. Pickett, Phys. Rev. B 41 (1992) 10437.
[13] G. Lehmann, M. Taut, Phys. Status Sol. B 87 (1978) 221.
[14] P. Lagrange, D. Bégin, C. Hérold, J.F. Marêché, Images de la Recherche, Départements Sciences Physiques et Mathématiques et Sciences Chimiques du CNRS Les Fullerènes 66 (1997) J. Moscovici, thèse de l'Université Paris VI, 1994.
[15] O. Chauvet, L. Forro, J.R. Cooper, G. Mihaly, A. Janossy, Synth. Metals 70 (1995) 1333.

[16] V. Brouet, H. Alloul, Y. Yoshinari, L. Forro, Phys. Rev. Lett. 76 (1996) 3638.
[17] P. Suortti, Th. Buslaps, P. Fajardo, V. Honkimäki, M. Kretzchmer, U. Lienert, J.E. McCarthy, M. Renier, Th. Tschentscher, T. Meinander, J. Synchrotr. Radiat. 6 (1999) 69.
[18] F. Balibar, Y. Epelboin, C. Malgrange, Acta Crystallgr. A 31 (1975) 836;
E. Erola, V. Eteläniemi, P. Suortti, P. Pattison, W. Thomlinson, J. Appl. Cryst. 23 (1990) 35.
[19] W.M. DuMond, Phys. Rev. 33 (1929) 643;
W.M. DuMond, Phys. Rev. 36 (1930) 146.
[20] F. Biggs, L.B. Mendelsohn, J.B. Mann, At. Data Nucl. Data Tables 16 (1975) 201.
[21] G. Loupias, J. Chomilier, D. Guérard, J. Phys. Lett. (Paris) 45 (1984) L301;
M.Y. Chou, S. Louie, M.L. Cohen, N. Holzwarth, Phys. Rev. B 30 (1984) 1062;
G. Loupias, J. Chomilier, D. Guérard, Solid State Commun. 55 (1985) 299.
[22] M.Y. Chou, M.L. Cohen, S.G. Louie, Phys. Rev. B 33 (1986) 6619;
S. Rabii, J. Chomilier, G. Loupias, Phys. Rev. B 40 (1989) 10105.